ISSN 1990-7931, Russian Journal of Physical Chemistry B, 2017, Vol. 11, No. 3, pp. 473–480. © Pleiades Publishing, Ltd., 2017.
Original Russian Text © A.V. Mokshin, B.N. Galimzyanov, 2017, published in Khimicheskaya Fizika, 2017, Vol. 36, No. 6, pp. 61–69.

DYNAMICS OF PHASE TRANSITIONS

Calculation of the Nucleation Barrier and Interfacial Free Energy of New-Phase Nuclei by the Thermodynamic Integration Method Using Molecular Dynamics Simulation Data

A. V. Mokshin[a, b, *] and B. N. Galimzyanov[a, b]

[a] *Institute of Physics, Kazan Federal University, Kazan, 420008 Russia*
[b] *Landau Institute for Theoretical Physics, Russian Academy of Sciences, Moscow, 119334 Russia*
**e-mail: anatolii.mokshin@mail.ru*

Received September 7, 2016

Abstract—An approach to determining the nucleation barrier and interfacial free energy (surface tension) based on molecular dynamics simulations of structural transformations, in particular, the formation of new phase nuclei, is reported. The approach is based on the thermodynamic integration method, wherein key elements are trajectories characterizing the potential energy change, which are obtained from independent numerical experiments. An important feature of the approach is its applicability to both equilibrium and nonequilibrium systems, as well as the possibility of determining the above thermodynamic characteristics for small new-phase nuclei, with a significant curvature of the surface. For example, we present the temperature dependencies of the surface tension of water droplet nuclei for water vapor nucleation and of the nucleation barrier to crystal nucleation in two model glassy systems, which are computed within the framework of the proposed approach. The calculated values of the surface tension coefficient of water droplet nuclei are compared with the available experimental data.

Keywords: thermodynamic integration, molecular dynamics, nucleation barrier, free energy, surface tension
DOI: 10.1134/S1990793117030216

INTRODUCTION

With the development of methods for numerical modeling of equilibrium and nonequilibrium processes in many-particle systems, problems associated with interpreting simulation results and finding various physical parameters of such systems have become topical [1–6]. The specificity of simulations in *classical molecular dynamics*, associated with the possibility of obtaining information on the trajectories and velocities of the molecules (atoms) of the system, naturally ensured a fairly successful application of this simulation method to finding pair and many-particle distribution functions, temporal correlation functions, and spectral densities of correlation functions, which made it possible to compare simulation results with experimental data, in particular, in dielectric, neutron, and X-ray spectroscopies [7, 8]. Nevertheless, various thermodynamic parameters, such as free energy and configurational entropy are mostly calculated by techniques based on the Monte Carlo method [9], in which the characterization and statistical treatment of possible structural configurations of the system under specified external conditions are carried out fairly accurately. For example, the Monte Carlo simulation for replica exchange Markov chain [10] and umbrella sampling method, in which the Monte Carlo method is adapted to computation of the free energy as a function of a reaction coordinate, an order parameter, which allows one to determine the so-called energy landscape of the system [11, 12]. The difficulties in calculating the free energy by the Monte Carlo method arise for a system with strongly nonequilibrium effects [13].

Attempts to adapt simulations of molecular dynamics directly to solution of problems associated with determination of the free energy led to the emergence of a number of methods, notably metadynamics simulations, proposed and developed by M. Parinello's group [14, 15], and the thermodynamic integration method [16]. In the present work, we demonstrate that the thermodynamic integration method can be applied to calculating various thermodynamic parameters, such as the nucleation barrier and the interfacial free energy of the critically-sized nucleus of a new phase. Section 1 describes the thermodynamic integration method as applied to calculating the absolute values of the free energy. Sections 2 and 3 demonstrate how this method is applied to determining the nucleation barrier and interfacial free energy, respectively. Lastly, the results of molecular dynamics calculations of condensation of the water droplets and the

nucleation of crystals in model amorphous systems performed using this method are presented in Section 4.

1. APPLICATION OF THERMODYNAMIC INTEGRATION TO ESTIMATING THE FREE ENERGY

Let a system of N identical classical particles of the same mass m, confined in a certain volume V and interacting with each other through a pairwise additive spherical potential $u(r_{ij}) \equiv u_{ij}$, be in a state with temperature T and pressure P; i.e., an NPT ensemble is realized.[1] In accordance with classical mechanics, the coordinates $\mathbf{r}^{(i)}$ and momenta $\mathbf{p}^{(i)}$ $(i = 1,2,\ldots,N)$ of the particles form a $6N$-dimensional phase space,

$$A(\mathbf{r}^{(1)},\ldots,\mathbf{r}^{(N)},\mathbf{p}^{(1)},\ldots,\mathbf{p}^{(N)}),$$

a phase point in which defines the instantaneous state of the system. In the absence of the direct interaction of the particles with an external field, the Hamiltonian in a general form reads as [16]

$$H(\mathbf{r}^N,\mathbf{p}^N) = \sum_{i=1}^{N}\frac{|\mathbf{p}_i|^2}{2m} + \frac{1}{2}\sum_{i,j=1}^{N} u(r_{ij}).$$

The Gibbs energy of the system is defined as

$$G = U + PV - TS,$$

where U is the internal energy, V is the volume, and S is the entropy. On the other hand, the quantity

$$F = U - TS = -k_B T \ln Q_N \tag{1}$$

is the Helmholtz energy, where Q_N is the partition function integral:

$$\begin{aligned} Q_N &= \frac{1}{N!h^{3N}}\iint d\mathbf{p}^N d\mathbf{r}^N \exp\left\{-\frac{H(\mathbf{r}^N,\mathbf{p}^N)}{k_B T}\right\} \\ &= \frac{(3\pi m k_B T)^{3N/2}}{N!h^{3N}}\int d\mathbf{r}^N \exp\left(-\frac{u}{k_B T}\right), \end{aligned} \tag{2}$$

where $u = (1/2)\sum_{i,j=1}^{N} u(r_{ij})$. The second equality in expression (2) is obtained by integrating the exponential function with respect to the momenta; the remaining integral in this expression is known as the configuration integral [16].

Consider such a transformation (transition) of the system from some state I to state II, for which the temperature T, number of particles N, and volume V do not change, but the potential energy changes, and consequently, the free energy F does. Although the type of transition at the present stage of consideration is not specified (it can be a structural transition or relaxation to a certain equilibrium state), the following conditions are imposed on the nature of the transition: the transition must be reversible and not contain any signs of hysteresis, whereas the change of the free energy should occur continuously. Thus, this cannot be a first-order phase transition.

Let the transition of the system from a certain initial state I to state II be described by the dimensionless parameter λ, which can be, for example, an order parameter, a reaction coordinate, etc., such that

$$F^{\mathrm{I}} \equiv F^{\mathrm{I}}(\lambda = 0) \text{ and } u^{\mathrm{I}} \equiv u^{\mathrm{I}}(\lambda = 0) \text{ at } \lambda = 0,$$

$$F^{\mathrm{II}} \equiv F^{\mathrm{II}}(\lambda = 1) \text{ and } u^{\mathrm{II}} \equiv u^{\mathrm{II}}(\lambda = 1) \text{ at } \lambda = 1.$$

Then, taking (1) and (2) into account, we obtain

$$\begin{aligned} \frac{dF(N,V,T,\lambda)}{d\lambda} &= -\frac{k_B T}{Q(N,V,T,\lambda)}\frac{\partial Q(N,V,T,\lambda)}{\partial\lambda} \\ &= \int d\mathbf{r}^N \frac{\partial u(\lambda)}{\partial\lambda}\exp\left(-\frac{u(\lambda)}{k_B T}\right)\left[\int d\mathbf{r}^N \exp\left(-\frac{u(\lambda)}{k_B T}\right)\right]^{-1}. \end{aligned} \tag{3}$$

The last equality in (3) can be recast as

$$\frac{dF(N,V,T,\lambda)}{d\lambda} = \left\langle\frac{\partial u(\lambda)}{\partial\lambda}\right\rangle_\lambda, \quad \lambda \in [0,1], \tag{4}$$

where $\langle\ldots\rangle_\lambda$ means averaging over an ensemble of independent trajectories λ. Expression (4) defines the so-called thermodynamic integration procedure (λ-expansion), proposed by Kirkwood [16].

Expression (4) indicates first of all that the change in the free energy correlates with the change in the potential energy of a many-particle system, which in turn can be caused by transformations in the structure of the system or by a change in the interparticle interaction potential, for example, as a result of a chemical reaction. Further, as follows from (4), to estimate the change in the free energy of the system, it is sufficient to know the ensemble of trajectories $u_{ij}(\lambda)$ characterizing the change in the potential energy, which can be obtained based on independent experimental measurements, molecular dynamics simulations, Monte Carlo simulations or theoretical calculations.

Thermodynamic integration makes it possible to evaluate the absolute value of the free energy of state II, F^{II}, at a known value of the initial state:

$$F^{\mathrm{II}} = F^{\mathrm{I}} + \int_0^1 d\lambda\left\langle\frac{\partial u(\lambda)}{\partial\lambda}\right\rangle_\lambda,$$

where the integral is calculated numerically. For example, to estimate the absolute value of the free energy of the crystalline phase of a many-particle system with known interparticle interaction potential, it is convenient to consider an Einstein crystal as initial state I [17].

The crystallization of a supercooled liquid, melting of a superheated crystal, condensation of vapor, evap-

[1] The assumptions of pair-additive forces and a spherical potential make it possible only to simplify primary calculations, but are not necessary. Simulations can be performed with a potential of arbitrary form.

oration of a liquid, and some other processes are first-order phase transitions, and therefore, it is not possible to estimate the free energy change caused by these phase transitions directly by means of thermodynamic integration [13]. Nevertheless, it can be shown that the thermodynamic integration method can still be applied, albeit under certain conditions, to evaluating the characteristics of these processes, such as the work required for the system to form a critically-sized nucleus, nucleation barrier, and interfacial free energy of the critically-sized new-phase nucleus.

2. NUCLEATION BARRIER

According to the classical concepts [18], the formation of new-phase nuclei is an activation-type process. This means that the nucleus becomes stable only after reaching a certain critical size n_c; energy required to form such a nucleus is [18–20]

$$\Delta F(n_c) = F^{\mathrm{II}} - F^{\mathrm{I}} = \alpha_s \left(\frac{n_c}{\rho}\right)^{2/3} \sigma_s - |\Delta\mu| n_c,$$

where F^{I} is the free energy of the initial state of the system; F^{II} is the free energy of the system containing a new-phase nucleus of critical size n_c; α_s is the form factor of the surface of the nucleus (for example, for a spherical nucleus, $\alpha_s = (36\pi)^{1/3}$; for a cubical nucleus, $\alpha_s = 6$; etc.); ρ is the number density of phase II; σ_s is the interfacial free energy; $\Delta\mu$ is the difference between the chemical potentials of phases I and II. Let the belonging of the particles of the system to one or another phase be known. If the particles in state I are distributed uniformly throughout the system, thereby forming a certain common phase, then we can write

$$u^{\mathrm{I}} = \mathrm{N}u_{\mathrm{I}},$$

where $u^{\mathrm{I}} \equiv u^{\mathrm{I}}(\lambda = 0)$ and u^{I} is the mean potential energy of state I per particle. Let the system in some state with $0 < \lambda \le 1$ contain a new-phase nucleus of size $n \le n_c$, then, the potential energy of the particles of the system can be estimated as

$$u = (N - n)u_{\mathrm{I}} + nu_{\mathrm{II}}.$$

Here, $u \equiv u(\lambda)$ and u_{II} is the mean potential energy of phase II per particle. Since the considered transition $\mathrm{I} \to \mathrm{II}$ is associated with the formation of the critically-sized nucleus n_c, it is convenient to relate the parameter λ with the nucleus size as

$$\lambda = \left(n/n_c\right)^{1/3}.$$

Then,

$$u(\lambda) = (N - \lambda^3 n_c)u_{\mathrm{I}} + \lambda^3 n_c u_{\mathrm{II}} = \mathrm{N}u_{\mathrm{I}} + \lambda^3 n_c(u_{\mathrm{II}} - u_{\mathrm{I}}).$$

Hence,

$$\Delta F = F^{\mathrm{II}}(\lambda = 1) - F^{\mathrm{I}}(\lambda = 0) = \int_0^1 \left\langle \frac{\partial u(\lambda)}{\partial \lambda} \right\rangle_\lambda d\lambda. \quad (5)$$

Thus, if only a single critically-sized nucleus is formed in the considered system, which is possible under certain thermodynamic conditions [20], and the nucleation process itself satisfies the conditions of the NVT ensemble, then the value of the nucleation barrier can be estimated using expression (5). Here, the input parameters are trajectories characterizing the change in the potential energy during nucleation, as well as trajectories of growth of the new phase nucleus, $n(t)$ at $n \le n_c$, quantities obtained from molecular dynamics simulations. In this case, the averaging $\langle \ldots \rangle_\lambda$ is performed over various molecular-dynamics iterations.

3. INTERFACIAL FREE ENERGY

The interfacial free energy σ_s can be directly measured through determining the pressure anisotropy in the surface layer:

$$\sigma_s \backsim \left(P_{zz} - \frac{P_{xx} + P_{yy}}{2}\right), \quad (6)$$

where the z axis coincides with the normal to the surface; P_{xx}, P_{yy}, and P_{zz} are the diagonal components of the pressure tensor. Clearly this approach is applicable if the interface is formed by a macroscopic object, in the surface layer of which, it is possible to uniquely determine the normal and tangential directions and if the corresponding components of the pressure tensor are measurable. Expression (6) is also used to find σ_s from molecular dynamics simulation data when considering an idealized system consisting of two coexisting phases with a flat interface. In this case, the components of the pressure tensor are calculated using the Irwin–Kirkwood microscopic formulation [16].

At present, the interfacial free energy is commonly determined from molecular dynamics simulations by using various versions of the thermodynamic integration method [21, 22] and the method for estimating the characteristics of the thermal fluctuations of the surface within the framework of the capillary-wave model [23, 24]. However, in both methods, it is assumed that there is an extensive interface: in the first method, the interface should approximate a plane shape, whereas in the second, the interphase interface must be uniquely determined and have a size sufficient for a statistical characterization of its curvature. Thus, application of these methods to calculating the interfacial energy of microscopic objects, such as nuclei of a nascent phase, is difficult [25]. Nevertheless, it can be shown that the thermodynamic integration method can be used to estimate σ_s for critically-sized nuclei.

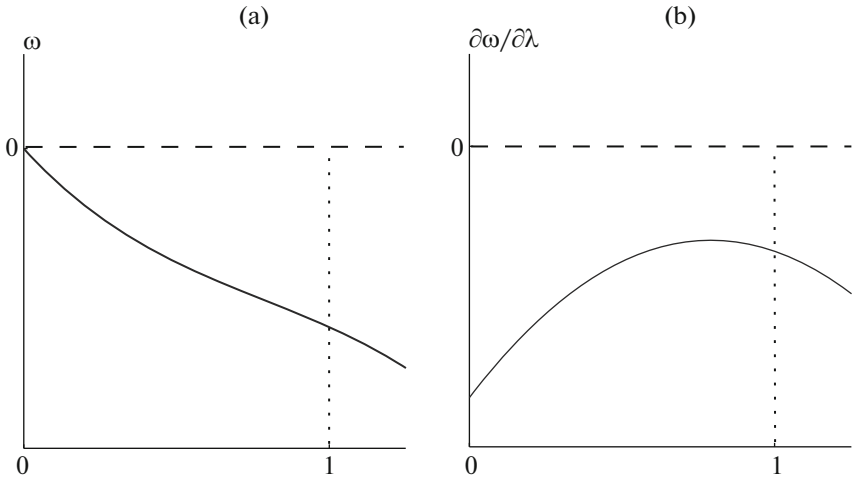

Fig. 1. (a) Curve showing how the surface energy $\omega(\lambda)$ of the nucleus changes in the course of its growth; (b) the derivative $\partial\omega(\lambda)/\partial\lambda$, obtained by numerical differentiation of the $\omega(\lambda)$ dependence. To perform thermodynamic integration, it is necessary to generate a $\partial\omega(\lambda)/\partial\lambda$ set, which can be done based on the results of a sequence of independent molecular dynamics iterations. After appropriate averaging, the integral in expression (7) is also calculated numerically.

In this case, the implementation of this method differs from the way it is realized in the known methods.

As it is known, the interfacial energy ω can be defined as the excess energy per unit surface area, which arises because of a lack of "neighbors" around surface particles in comparison with particles in the bulk [18]. Taking into account the neighbors of each particle only within the first coordination sphere yields [18]

$$\omega = \frac{1}{2}u(\hat{r}_{ij})(z - z')n',$$

where $\hat{r}_{ij}$ is the average distance between neighboring particles of the daughter phase; n' is the number of surface particles per unit area; z and z' the first coordination numbers for the bulk and surface particles, respectively. In general, the quantity ω is a function of the nucleus size. Then, in accordance with expression (5), the interfacial free energy can be estimated as

$$\sigma_s = -\int_0^1 \left\langle \frac{\partial\omega}{\partial\lambda} \right\rangle_\lambda d\lambda. \qquad (7)$$

The parameter λ, as in calculating the nucleation barrier, can be conveniently related to the reduced size of the nascent nucleus, $\lambda = (n/n_c)^{1/3}$. With this definition, the parameter λ is zero if there are no new-phase nuclei in the system, and therefore, there is no interphase interface; whereas $\lambda = 1$ if the size of the nucleus is equal to the critical size n_c. In processing the results of molecular dynamics simulations, the symbol $\langle\ldots\rangle_\lambda$ means the averaging over an ensemble of independent trajectories at a specific value of λ [25]. In this method, the input parameters are the interfacial energy and the set of independent trajectories $n(t)$ ($n \le n_c$) that characterizes the growth of the nucleus. In this case, the coordination numbers z and z' can be conveniently determined from the results of molecular dynamics simulations as the surface area under the first peaks in the radial distribution functions for bulk and surface particles [16]:

$$z = 4\pi\rho\int_0^{r_{\min}} r^2 g_v(r)dr,$$

$$z' = 4\pi\rho\int_0^{r_{\min}} r^2 g_s(r)dr,$$

where $r_{\min}$ is the position of the first minimum in the corresponding radial distribution of particles and ρ is the number density of particles.

Figure 1a shows, as an example, a curve characterizing the change in the interfacial energy $\omega(\lambda)$ ($\lambda = (n/n_c)^{1/3}$) of an individual nascent nucleus obtained from molecular dynamics simulations of the nucleation process. The derivative $\partial\omega(\lambda)/\partial\lambda$ corresponding to this curve, calculated numerically, is displayed in Fig. 1b.

RESULTS

4.1. Crystallization of Model Glassy Systems: the Barrier to Crystal Nucleation

Molecular dynamics calculations of the process of crystal nucleation in two different glassy systems, differing in the interparticle interaction potentials, were performed. The initial configuration of each simulated

system was specified in the form of a fcc lattice inside a cubic cell of size $20.3\sigma \times 20.3\sigma \times 20.3\sigma$, where σ is the interparticle interaction potential parameter characterized the effective particle size. Periodic boundary conditions were imposed on the simulation cell in all directions. Further, $N = 6912$ particles were located at the crystal lattice sites. All the calculations were performed for the NPT ensemble; the equations of motion were integrated out in accordance with the Verlet velocity algorithm with an integration step of $\Delta t = 0.005\tau$. Initially, each simulated system was transferred into the liquid state. Its temperature was set much higher than the melting point T_m, and in this state, the system was equilibrated. Next, glassy-state samples were prepared by rapid cooling at a rate of $dT/dt = 0.001\varepsilon/k_B\tau$, where ε is the interparticle interaction parameter characterizing the depth of the potential well, $\tau = \sigma(m/\varepsilon)^{1/2}$ is the time unit, and m is the mass of the particle.[2] The temperature and pressure were controlled using the Nosé–Hoover thermostat and barostat with the parameters $Q_T = 50\varepsilon\tau^2$ and $Q_P = 100\varepsilon\tau^2$. To enable subsequent statistical treatment of molecular dynamics simulation results within the framework of the thermodynamic integration method, 50 samples were prepared for each (P,T) considered thermodynamic state. The detection of local ordered groups of particles was performed using cluster analysis by the Wolde–Frenkel algorithm [26], capable of examining the nearest environment of each particle.

For example, in the first system, the particles interacted through the Dzugutov oscillating short-range pair potential [27]. In solid-state, this system (Dzugutov system) forms predominantly quasi-crystalline phases and a crystalline phase with a fcc lattice [28]. Amorphous samples were prepared for states with temperatures $T = 0.05, 0.1, 0.15, 0.3$, and $0.5\varepsilon/k_B$ at a constant pressure of $P = 14\varepsilon/\sigma^3$. For the given isobar, the melting point is $T_m \approx 1.51\varepsilon/k_B$, whereas the glass-transition temperature (at the selected cooling rate) is $T_g \approx 0.65\varepsilon/k_B$ [29].

The second system is a two-component Lennard-Jones system, where the correspondence between the Lennard-Jones parameters for particles of types α and β were determined by applying the so-called mixing rules, which have the form

$$\begin{gathered}\sigma_{\beta\beta} = 0.8\sigma_{\alpha\alpha},\\ \sigma_{\alpha\beta} = (\sigma_{\alpha\alpha} + \sigma_{\beta\beta})/2,\\ \varepsilon_{\beta\beta} = 0.5\varepsilon_{\alpha\alpha},\\ \varepsilon_{\alpha\beta} = \varepsilon_{\alpha\alpha} + \varepsilon_{\beta\beta},\\ \sigma \equiv \sigma_{\alpha\alpha},\\ \varepsilon \equiv \varepsilon_{\alpha\alpha},\\ m = m_\alpha = m_\beta = 1.\end{gathered} \tag{8}$$

The concentration of particles of type α was 80% of their total number. It should be noted that mixing rules (8) differ from those, which are usually used to produce known glass-forming two-component Lennard-Jones systems: the Kob-Anderson system and the Wahnstrom system. For the system under study, the amorphous samples were prepared at temperatures $T = 0.01, 0.05, 0.1, 0.2$, and $0.3\varepsilon/k_B$ for states with a pressure of $P = 17\varepsilon/\sigma^3$. The melting point was $T_m \approx 1.65\varepsilon/k_B$ and the glass transition temperature was estimated as $T_g \approx 0.92\varepsilon/k_B$ [30].

As was shown [30] at specified (P,T)-conditions, the crystallization of both glassy systems is initiated through the mechanism of homogeneous crystal nucleation. At the same time, sufficiently high pressures ($P = 14\varepsilon/\sigma^3$ and $17\varepsilon/\sigma^3$ for the Dzugutov and Lennard-Jones systems, respectively) impart specific features to the process of structural ordering. First, the appearance of individual crystal nucleus is detected on the space–time scales realized in molecular dynamics calculations. The critical size is very small: for the states examined, it was found that the value of n_c does not exceed 100 and 60 particles for the Dzugutov and Lennard-Jones systems, respectively, although the crystallization of the systems proceeds very slowly due to high viscosity. Secondly, under such conditions, the volume of the system practically does not change during nucleation.

The small size and isolation of the nucleus make it possible to select in the simulation cell a local region that contains only one nucleus (for example, the largest) and evaluate the nucleation barrier by the thermodynamic integration method (Section 2). The values of the nucleation barrier obtained for the Dzugutov glassy system and two-component Lennard-Jones glassy system at various temperatures are shown in Fig. 2. As can be seen from this figure, the value of ΔF in the temperature range covered has the same linear temperature dependence for both systems, in agreement with the classical theory of nucleation [31]. Further, according to the classical theory of nucleation, the free energy change ΔF is expressed through the temperature of the system, the critical size, and the Zel'dovich parameter Z:

$$\Delta F \backsim k_B T (n_c Z)^2.$$

[2] At $\sigma = 0.34$ nm, $\varepsilon/k_B = 120$ K, and $m \approx 6.6 \times 10^{-26}$ kg (k_B is the Boltzmann constant), corresponding to the argon atom, we have $\tau \approx 10^{-12}$ s and $dT/dt \approx 10^{11}$ K/s).

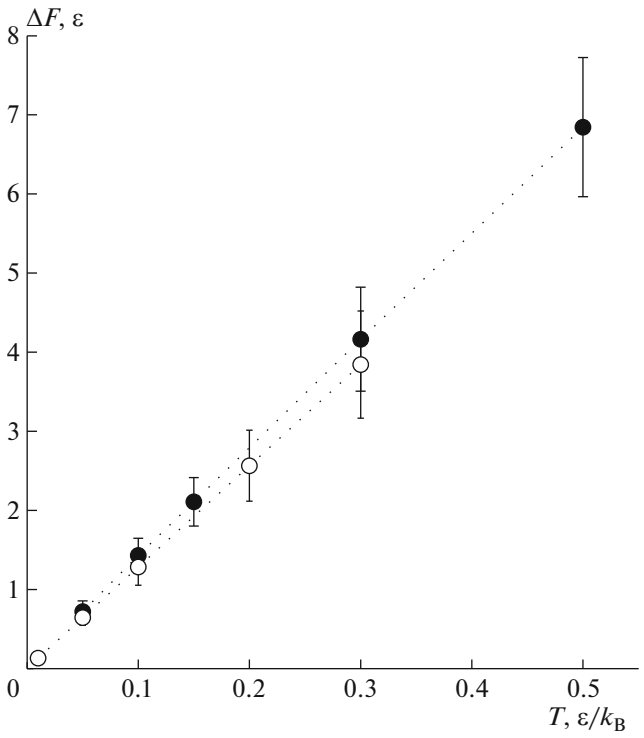

Fig. 2. Temperature dependence of the nucleation barrier calculated by the thermodynamic integration method from the results of molecular dynamics simulations for the Dzugutov system (●) and two-component Lennard-Jones system (○). The averaging in (5) was performed using the results of 50 independent molecular dynamics iterations.

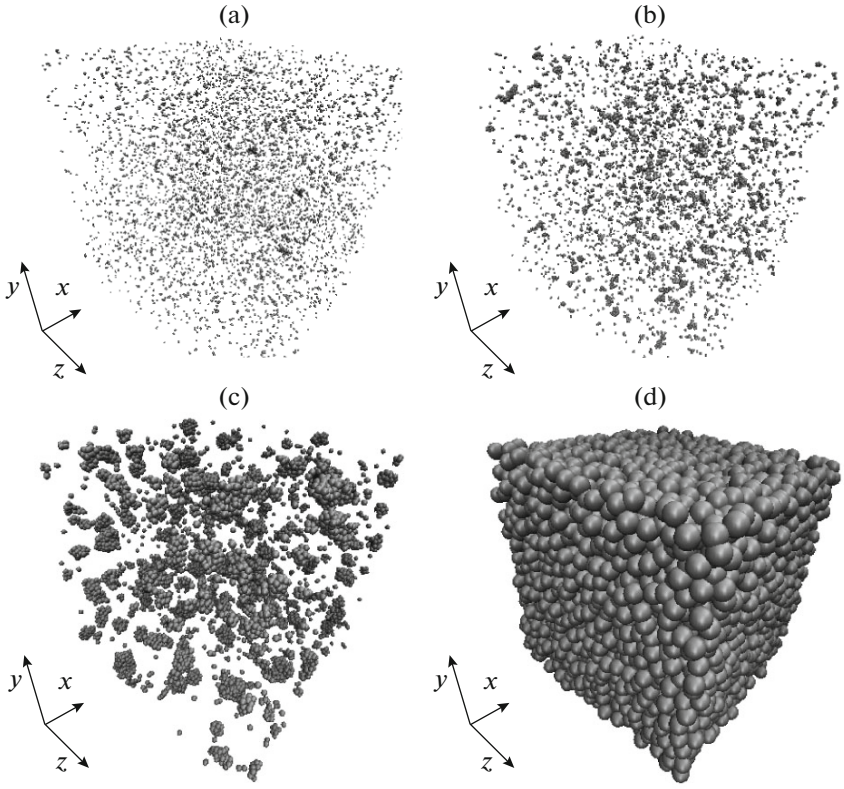

Fig. 3. Configurations of the simulated system (condensing water vapor) at a temperature of 273 K, a pressure of $P = 1$ atm and at different time: (a) 0.2 ns, (b) 0.6 ns, (c) 1.0 ns, and (d) 1.2 ns. The scale of the region shown in the figures decreases from case a to case b.

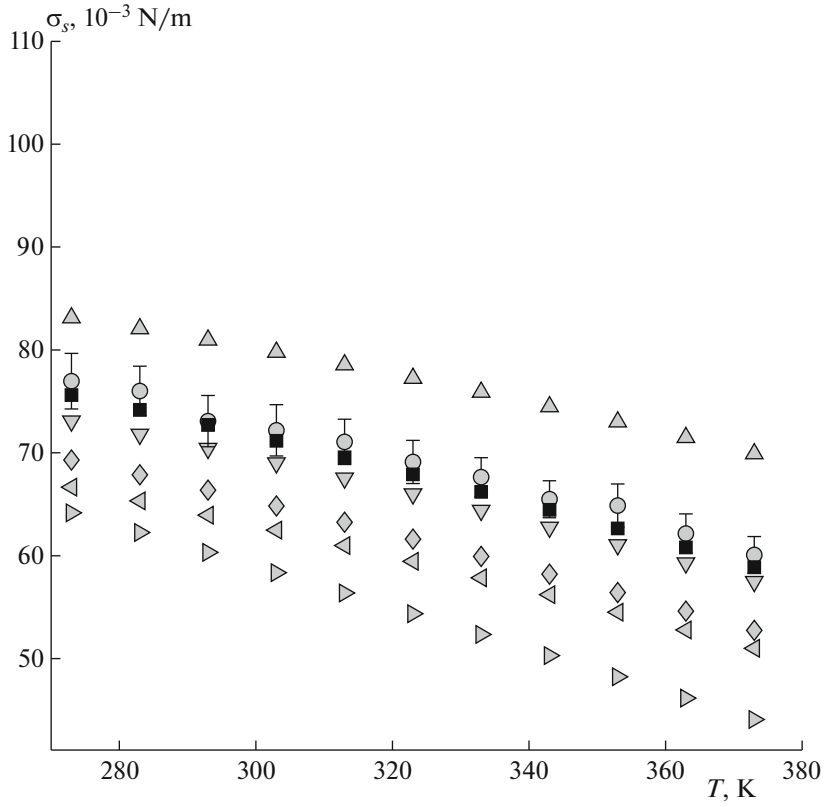

Fig. 4. Temperature dependence of the surface tension σ_s. The squares represent the experimental values of the surface tension of water for a macroscopic (flat) interface [36]. The circles represent the values of σ_s for critically-sized water droplets obtained from molecular dynamics simulations by using the thermodynamic integration method. The other points represent the surface tension values obtained from Monte Carlo simulations based on the SPC/E and TIP4P atomistic water models of various modifications: (△) TIP4P/Ice, (◇) TIP4P/Ew, (▽) TIP4P/2005, (▷) TIP4P, and (◁) SPC/E.

Thus, although the critical size n_c of the crystal nucleus tends to decrease with increasing depth of supercooling (decreasing temperature of the system), the change in n_c is almost completely compensated by the increase of the Zel'dovich parameter with decreasing temperature of the system. For example, the method of inverted averaging, described in detail in [25, 30], was applied to estimate the value of Z, which was found to decrease with increasing temperature from 0.014 to 0.011 for the Dzugutov system and from 0.028 to 0.020 for the Lennard-Jones system.

4.2. Condensation of Water Vapor: the Surface Tension of the Critically-Sized Water Droplets

Molecular dynamics simulations of the condensation of water vapor was performed for a system consisting of 8000 water molecules enclosed in a cubic cell with periodic boundary conditions and interacting with each other through an effective potential, a modification of the Stillinger–Weber potential [32, 33]. The volume of cell is $V = L^3$, where $L \approx 466$ Å. The equations of motion were integrated using the Verlet algorithm with a time step of $\Delta t = 1$ fs. The starting samples of equilibrated vapor were cooled at a rate of $dT/dt = 10$ K/ns to states corresponding to temperatures 273–373 K. The subsequent molecular dynamics simulations were performed in the NPT ensemble mode (at atmospheric pressure). The temperature and pressure of the system were controlled using the Nosé–Hoover thermostat and barostat with $Q_T = Q_P = 10$ (kcal fs^2)/mol [25]. "Bound" molecules tending to form the liquid phase were detected by calculating the Stillinger criterion for all pairs of neighboring molecules. According to this criterion, two molecules can be considered bound if the distance between their centers of mass is $r_{ij} \le 3.56$ Å [25, 34].

Figure 3 displays fragments of the simulated system (supercooled water vapor) at a temperature of 273 K at different instants of time; only molecules forming the liquid phase are shown. As can be seen, the condensation of vapor occurs through the formation of new-phase (liquid) nuclei, proceeding according to a homogeneous scenario: the probability of formation of a drop nucleus does not depend on the position (coordinates) in the cell. Figures 3a and 3b show sub-

critically-sized droplets ($n < n_c$). Figure 3c shows a system containing critically-sized nuclei. The critical size n_c was determined by statistical treatment of the simulation results using the mean-first-passage-time method [35]. For example, for this system at 273 K and atmospheric pressure, the size of the critically-sized nucleus was $n_c = 75 \pm 25$ molecules. Figure 3d displays fragment of liquid system at time 1.2 ns.

Figure 4 compares the surface tension of the critically-sized nucleus of water droplets calculated by the thermodynamic integration method (Section 3) from molecular dynamics simulation data and with the experimental data reported in [36] and with the results of Monte Carlo simulations based on the SPC/E (three-point) and TIP4P (four-point) atomistic models of water [37–40]. As can be seen from Fig. 4, the values of the surface tension coefficient obtained in the present study are in close agreement with the experimental data over the entire temperature range covered. Note that this agreement between the present simulation results and the experimental data is somewhat unexpected for two reasons. First, as indicated above, molecular dynamics calculations were performed with an effective intermolecular interaction potential, a factor that should lead to more inaccurate results as compared to predictions of atomistic models. The second reason is related to the dependence of the surface tension on the geometry of the surface. Clearly, the surface of droplet nuclei comprised of less than hundreds of molecules is strongly curved. Nevertheless, in the absence of proper experimental data, the surface tension of droplet nuclei is compared to that of a planar surface.

ACKNOWLEDGMENTS

Molecular dynamics calculations were performed at the computer cluster of the Kazan Federal University and at the computer cluster of the Interagency Supercomputer Center of the Russian Academy of Sciences.

The work was supported in part by the Russian Foundation for Basic Research, project no. 14-02-0335.

REFERENCES

1. Yu. K. Tovbin, *The Molecular Theory of Adsorption in Porous Solids* (Fizmatlit, Moscow, 2012; CRC, Boca Raton, FL, 2017).
2. A. G. Grivtsov, *Molecular Dynamics Method in Physical Chemistry,* Ed. by Yu. K. Tovbin (Nauka, Moscow, 1996) [in Russian].
3. G. G. Malenkov, Colloid. J. **72**, 653 (2010).
4. G. G. Malenkov, J. Struct. Chem. **54**, S252 (2013).
5. S. V. Shevkunov, Khim. Fiz. **22** (1), 90 (2003).
6. V. S. Neverov and A. V. Komolkin, Russ. J. Phys. Chem. B **4**, 217 (2010).
7. B. J. Berne and G. D. Harp, Adv. Chem. Phys. **17**, 63 (1970).
8. A. V. Mokshin, Theor. Math. Phys. **183**, 449 (2015).
9. G. M. Torrie and J. P. Valleau, Chem. Phys. Lett. **28**, 578 (1974).
10. R. H. Swendsen and J. S. Wang, Phys. Rev. Lett. **57**, 2607 (1986).
11. R. M. Lynden-Bell, J. S. van Duijneveldt, and D. Frenkel, Mol. Phys. **80**, 80 (1993).
12. J. S. van Duijneveldt and D. Frenkel, J. Chem. Phys. **96**, 4655 (1992).
13. S. Jungblut and C. Dellago, Eur. Phys. J. E **39**, 77 (2016).
14. A. Laio and M. Parrinello, Proc. Natl. Acad. Sci. USA **99**, 12562 (2002).
15. G. Bussi, A. Laio, and M. Parrinello, Phys. Rev. Lett. **96**, 090601 (2006).
16. J. P. Hansen and I. R. McDonald, *Theory of Simple Liquids* (Academic, London, 2006).
17. D. Frenkel and B. Smit, *Understanding Molecular Simulation* (Academic, San Diego, 2001).
18. Ya. I. Frenkel', *Kinetic Theory of Liquids* (Nauka, Moscow, 1975) [in Russian].
19. V. M. Fokin, E. D. Zanotto, N. S. Yuritsyn, and J. W. P. Schmelzer, J. Non-Cryst. Solids **352**, 2681 (2006).
20. D. Kashchiev, *Nucleation: Basic Theory with Applications* (Butterworth-Heinemann, Frenkel Oxford, 2000).
21. J. Q. Broughton and G. H. Gilmer, J. Chem. Phys. **84**, 5759 (1986).
22. R. L. Davidchack and B. B. Laird, Phys. Rev. Lett. **85**, 4751 (2000).
23. D. I. Zhukhovitskii, Colloid. J. **72**, 188 (2010).
24. F. P. Buff, R. A. Lovett, and F. H. Stillinger, Phys. Rev. Lett. **15**, 621 (1965).
25. A. V. Mokshin and B. N. Galimzyanov, J. Phys. Chem. B **116**, 11959 (2012).
26. P. R. ten Wolde, M. Ruiz-Montero, and D. Frenkel, J. Chem. Phys. **104**, 9932 (1996).
27. M. Dzugutov, Phys. Rev. Lett. **70**, 2924 (1993).
28. A. V. Mokshin and J.-L. Barrat, J. Chem. Phys. **130**, 034502 (2009).
29. A. V. Mokshin, B. N. Galimzyanov, and J.-L. Barrat, Phys. Rev. E **87**, 062307 (2013).
30. A. V. Mokshin and B. N. Galimzyanov, J. Chem. Phys. **142**, 104502 (2015).
31. V. P. Skripov, *Metastable Liquid* (Nauka, Moscow, 1972) [in Russian].
32. E. B. Moore and V. Molinero, J. Chem. Phys. **130**, 244505 (2009).
33. E. B. Moore and V. Molinero, Nature **479**, 506 (2011).
34. F. Stillinger and T. A. Weber, Phys. Rev. B **31**, 5262 (1985).
35. A. V. Mokshin and B. N. Galimzyanov, J. Chem. Phys. **140**, 024104 (2014).
36. H. White and J. V. Sengers, IAPWS Release on Surface Tension of Ordinary Water Substance (IAPWS, 2014). http://www.iapws.org/relguide/Surf-H2O-2014.pdf.
37. W. L. Jorgensen, J. Chandrasekhar, J. D. Madura, et al., J. Chem. Phys. **79**, 926 (1983).
38. H. W. Horn, W. C. Swope, and J. W. Pitera, J. Chem. Phys. **120**, 9665 (2004).
39. J. L. F. Abascal, E. Sanz, R. G. Fernandez, and C. Vega, J. Chem. Phys. **122**, 234511 (2006).
40. J. L. F. Abascal and C. Vega, J. Chem. Phys. **123**, 234505 (2005).

Translated by V. Smirnov